Title

Formation of Chlorine in the Atmosphere by Reaction of Hypochlorous Acid with Seawater.

Journal

Journal of Physical Chemistry Letters, 15(2)

Authors

Mandal, Imon
Karimova, Natalia
Zakai, Itai
et al.

Publication Date

2024-01-18

DOI

10.1021/acs.jpclett.3c03035

Peer reviewed

THE JOURNAL OF PHYSICAL CHEMISTRY LETTERS
A JOURNAL OF THE AMERICAN CHEMICAL SOCIETY

pubs.acs.org/JPCL
Letter

Formation of Chlorine in the Atmosphere by Reaction of Hypochlorous Acid with Seawater

Imon Mandal, Natalia V. Karimova, Itai Zakai, and R. Benny Gerber*

Cite This: J. Phys. Chem. Lett. 2024, 15, 432−438
Read Online

ABSTRACT: The highly reactive dihalogens play a significant role in the oxidative chemistry of the troposphere. One of the main reservoirs of these halogens is hypohalous acids, HOX, which produce dihalogens in the presence of halides (Y^-), where X, Y = Cl, Br, I. These reactions occur in and on aerosol particles and seawater surfaces and have been studied experimentally and by field observations. However, the mechanisms of these atmospheric reactions are still unknown. Here, we establish the atomistic mechanism of $HOCl + Cl^- \rightarrow Cl_2 + OH^-$ at the surface of the water slab by performing ab initio molecular dynamics (AIMD) simulations. Main findings are (1) This reaction proceeds by halogen-bonded complexes of $(HOCl)\cdots(Cl^-)_{aq}$ surrounded with the neighboring water molecules. (2) The halogen bonded $(HOCl)\cdots(Cl^-)_{aq}$ complexes undergo charge transfer from Cl^- to OH^- to form transient Cl_2 at neutral pH. (3) The addition of a proton to one proximal water greatly facilitates the Cl_2 formation, which explains the enhanced rate at low pH.

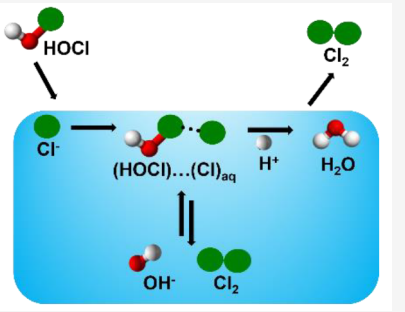

Reactive halogen species (RHS such as X, XY, and XO, where X, Y = Cl, Br, or I) play an important role in the chemistry and oxidizing capacity of the troposphere as well as stratosphere.[1−7] Firstly, the RHS act as an effective sink for ozone (O_3) by depleting O_3 through efficient catalytic cycles. Second, they influence the nitrogen oxides (NO_x), and HO_x cycles.[4−6] RHS also impact the lifetimes of reduced trace gases such as methane, non-methane volatile organic compounds, and dimethyl sulfide, as well as mercury in the atmosphere.[1,4,8] These RHS originate from different sources, including organohalogen oxidation,[1] ozone deposition to the ocean surface,[9] and release from sea salt aerosols.[5,7,10] The release occurs via the uptake of hypohalous acid species (HOX, where X is equal to Br, Cl, or I) from the gas phase[11] or hydrolysis of N_2O_5 forming $ClNO_2$[12] or hydrolysis of XNO_3 forming HOX.[6] However, alternation of atmospheric acidity due to changes in acid precursor gases emissions influence the RHS formation.[13] In fact, halogen formation gets promoted by the acid-driven reactions[14−16]

$$HOX + Y^- + H^+ \rightarrow XY + H_2O \ (X, Y = Cl, Br, \text{and } I) \quad (R1)$$

In these reactions, the protons (H^+) are incorporated into the reaction products formed, leading to acid-driven reactions. Sea salt aerosols originate at the same pH as seawater (∼8) but, within minutes, undergo a pH drop of a few pH units.[17] However, the value of pH ∼ 8 is an average value, and there are many conditions where locally seawater is acidic. The roles of seawater, aerosols, and the acidity of those media in halogen activation in the atmosphere, however, remain poorly understood and need to be addressed to further advance our understanding of the complex role of acidity in the atmosphere.

Among halogens, Cl contributes for 5.4−11.6% of total methane sinks and involved to a lesser extent for ozone destruction.[18] Additionally, chloride (Cl^-) is the greatest abundant halide anions in seawater, aerosol and most aqueous systems in the atmosphere.[4] However, the mechanisms responsible for the oxidation of Cl^- to reactive forms (e.g., $Cl^•$, ClO, Cl_2, BrCl, HOCl, and $ClNO_2$) are incompletely investigated.[19] Consequently, assessing the impacts of reactive chlorine on atmospheric chemistry become challenging. On the other hand, Cl is also used globally as chemical oxidant for drinking water disinfection due to its cost effectiveness. During water treatment, hypochlorous acid (HOCl) acts as the major reactive form among the different seawater like Cl species and most of the elementary oxidation of halides (Y^- where Y = Cl, Br, and I) reactions start with HOCl.[20] Another important fate of HOCl in the atmosphere is the heterogeneous reaction with halide anions in or on condensed aqueous phases, such as sea salt aerosol particle surfaces or seawater surfaces (R1) forming Cl_2 followed by photolysis generation of RHS Cl radicals. This heterogeneous reaction becomes faster in acidic environment as found in the laboratory experiments[21] and recently observed

Received: October 30, 2023
Revised: December 16, 2023
Accepted: December 20, 2023
Published: January 8, 2024

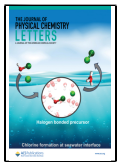

https://doi.org/10.1021/acs.jpclett.3c03035
J. Phys. Chem. Lett. 2024, 15, 432−438

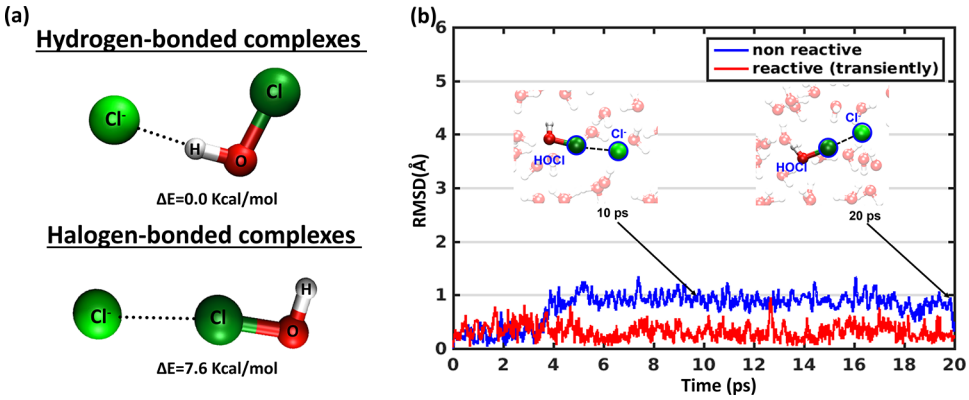

Figure 1. (a) Gas phase optimized structure (B3LYP/def2-TZVPD) of the hydrogen and halogen bonded pre-reactive complexes of (HOCl)···(Cl^-). (b) RMSD of the halogen bonded (HOCl)···$(Cl^-)_{aq}$ complexes (4 atoms H, O, Cl and Cl^-) along the time trajectory shows the complexes are stable at least 20 ps. Non-reactive legend indicate one representative trajectory among 7 trajectories which remain unreactive during simulations. Reactive demonstrates data from one representative trajectory among 3 trajectories which show transient reactions depicted in next section. Snapshots of the halogen bonded (HOCl)···$(Cl^-)_{aq}$ complexes at time 10 and 20 ps for representative unreactive simulation are shown in the inset.

in field studies.[19,22] Despite its importance, the atomistic details for these atmospheric important reactions with water medium have not been established until date. Thus, in this communication we aim to investigate the chemical pathway and role of water medium for HOCl reacting with the most abundant halide Cl^-, providing valuable insights about the formation of dihalogen Cl_2 in the atmosphere.

We develop a minimalistic computational model with (HOCl)···$(Cl^-)_{aq}$ complex and water slab containing 72 water molecules[23−25] to gain microscopic insight into the structures of the pre-reactive complexes, their lifetimes and the mechanisms of the reaction.[26] There are two possible orientations for the HOCl and Cl^- molecules to form the pre-reactive complexes: (a) the hydrogen bonded complex, in which the HOCl donates a hydrogen bond to Cl^- (b) the halogen bonded complex, in which the Cl^- acts as a nucleophile to the slightly electrophilic area on the Cl atom of HOCl. Our model unravels that halogen bonded complexes of the (HOCl)···$(Cl^-)_{aq}$ system play the major role in the dihalogen formation. The importance of halogen bonded complexes have also been reported for the halogen exchange reaction in (HOCl)···$(I^-)_{aq}$ and were explored spectroscopically.[27] Here, with AIMD simulations, we report the microscopic details of Cl_2 formation at acidic pH. Interestingly, under neutral pH condition, although Cl_2 forms transiently, it was not released in the subsequent process.

Stability of (HOCl)···(Cl−)$_{aq}$ Complexes in Water. The reaction HOCl + Cl^- → Cl_2 + OH^- in/on aerosol or seawater is not expected to proceed in a ballistic way but through a formation of pre-reactive complex of (HOCl)···$(Cl^-)_{aq}$. Gas phase calculations suggest that two possible structures are feasible for the HOCl and Cl^- molecules to form the pre-reactive complexes: (a) the hydrogen bonded complexes[28] and (b) the halogen bonded complexes.[27] As the pre-reactive complexes allow the two reagents HOCl and Cl^- to interact before they react, the stability and lifetimes of these pre-reactive complexes greatly affect the reaction mechanism. To study the complexes in water, we have employed an ab initio model of liquid water slab with periodic boundary conditions, as described in detail in the Computational Methods section (*vide infra*). We substitute hydrogen atoms with deuterium to accommodate a larger time step for the simulations. We first calculate the gas phase optimized structure (geometric parameters of these structures are provided in Table S1), position on the water slab model and simulate the system for 20 ps (ps). All the simulations resulted in the formation of the halogen and hydrogen bonded (HOCl)···$(Cl^-)_{aq}$ pre-reactive complexes (Figures 1, S1, and S2). Figures 1b, S1, and S2 show the root mean square deviation (RMSD) changes, which is an overall average measure to track the evolution of the complex structure along an MD trajectory with respect to a reference structure (here gas phase structure). These figures indicate two significant results: (a) both the halogen and hydrogen bonded (HOCl)···$(Cl^-)_{aq}$ complexes do not dissociate in water for at least 20 ps (our simulation time). This stability does not pertain to the trajectories where reaction occurs. In transiently reacting trajectories, the complexes undergo temporary reactions and return to the complex form. (b) (HOCl)···$(Cl^-)_{aq}$ complexes are similar to the initial gas phase structure. The stability against dissociation is remarkable for hydrogen bonded complexes. However, the fluctuations in RMSD for the hydrogen bonded (HOCl)···$(Cl^-)_{aq}$ complexes are up to 3 Å (1 Å = 1×10^{-10} m) due to the competition of hydrogen bonding partner of HOCl between Cl^- and surrounding waters (Figure S2). Fluctuation of halogen bonded (HOCl)···$(Cl^-)_{aq}$ complexes are ∼1 Å except one trajectory where the HOCl dissociates from the complex (Figure S1). This stabilized water envelop provides enough lifetime to the halogen bonded complexes. We implemented geometrical criteria to determine the formation of hydrogen and halogen bonds:[29,30] a hydrogen bond is defined by an H−Cl^- distance smaller than 3.2 Å, and an ∠O−H···Cl^- angle larger than 140°. A halogen bond is defined by a Cl−Cl^- distance smaller than 3.5 Å and a ∠Cl^-...Cl−O angle which is larger than 130°. Although, the gas phase calculations reveal that hydrogen bonded (HOCl)···(Cl^-) is 7.6 kcal/mol (1 kcal/mol = 4.184 kJ/mol) more stable than the halogen bonded (HOCl)···(Cl^-) complex, in the presence of water both hydrogen and halogen bonded (HOCl)···$(Cl^-)_{aq}$ complexes exhibit a minimum lifetime of 20 ps. While, hydrogen bonded pre-reactive complexes have been recognized as significant players in the reaction mechanisms,[31,32] in this study, we shed light on the crucial role of halogen bonded (HOCl)···$(Cl^-)_{aq}$ complexes in the formation of atmospheric Cl_2. Interestingly, hydrogen bonded

https://doi.org/10.1021/acs.jpclett.3c03035
J. Phys. Chem. Lett. 2024, 15, 432−438

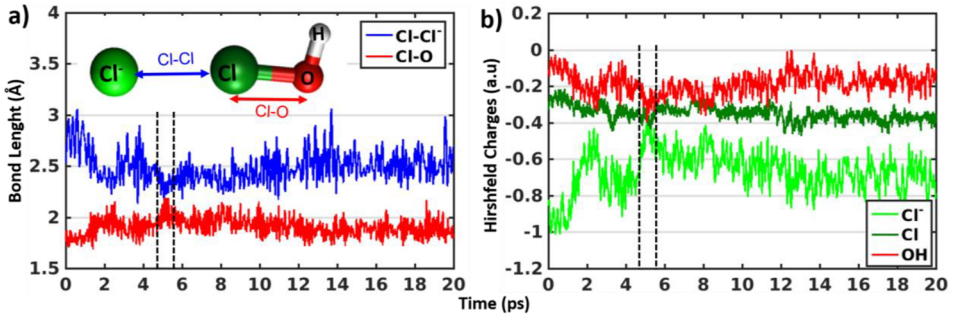

Figure 2. (a and b) Time evolution of the bond lengths (Cl−Cl$^-$ and Cl−O) and Hirshfeld partial charges (Cl$^-$, Cl, and summation of O and H from HOCl) of halogen bonded (HOCl)···$(Cl^-)_{aq}$ complexes along trajectory. The black dotted lines in parts a and b are eye guides for the time of the transient Cl_2 formation at neutral pH. Structure of the halogen bonded (HOCl)···$(Cl^-)_{aq}$ complexes (4 atoms H, O, Cl and Cl$^-$) with color coded bond lengths (for a) and atoms (for b) are provided in the inset of part a.

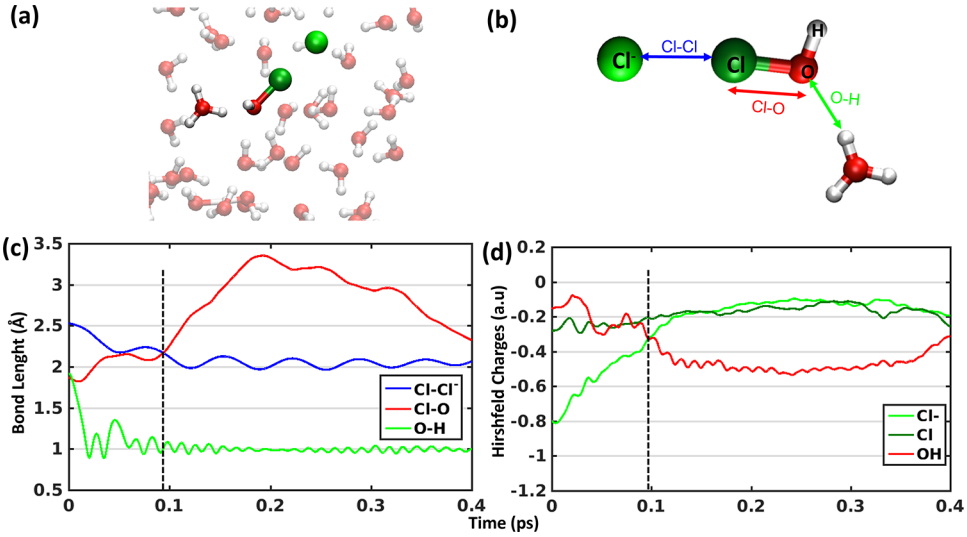

Figure 3. (a) Starting structure of halogen bonded (HOCl)···$(Cl^-)_{aq}$ complexes with the extra proton added on a neighboring water molecule forming hydronium ion. (b) Enlarged view of 4 atoms H, O, Cl and Cl$^-$ of (HOCl)···$(Cl^-)_{aq}$ complexes and the hydronium ion with color coded bond lengths (for c) and atoms (for d). (c and d) Time evolution of the bond lengths (Cl−Cl$^-$, Cl−O and O−H) and Hirshfeld partial charges (Cl$^-$, Cl and summation of O and H from HOCl) of halogen bonded (HOCl)···$(Cl^-)_{aq}$ complexes along trajectory. The black dotted lines in parts c and d are eye guides for the time of the non-reversible Cl_2 formation at acidic pH. Data for whole simulation are available in Figure S6.

complexes in all 5 simulations remain unreactive (Figure S3). Our simulations provide compelling evidence that halogen bonded (HOCl)···$(Cl^-)_{aq}$ complexes persist for a sufficient duration in water, serving as crucial precursors to the reaction.

Reaction of HOCl with Seawater Yield Transient Cl_2 Formation at Neutral pH. Although the overall RMSD demonstrate the stability of the halogen bonded (HOCl)···$(Cl^-)_{aq}$ complexes, time evolution of pairwise bond lengths of Cl−Cl$^-$ and Cl−O indicate transient formation of Cl_2 formation in 3 simulations at neutral pH. Figure 2a shows the time evolution of the bond lengths related to the Cl_2 formation reaction in one of the 3 transiently reactive simulations. The Cl−Cl$^-$ bond length decreases to 2.3 Å (blue) and the Cl−O bond length increases (red) at the same time (region between black lines) indicating the Cl_2 formation. The Hirshfeld partial charge analysis[33] also reveals the similar transition in the same time region around 5 ps (region between black lines). The partial charge on the Cl$^-$ (light green) ion was transferred to OH (red). Thus, the partial charge on Cl$^-$ increases, decreasing the charge of OH. Then, after 1 ps the Cl_2 falls apart and forms back halogen bonded (HOCl)···$(Cl^-)_{aq}$ complex. Data from the other 2 transiently reactive simulations are provided in Figure S4. The transient reaction times vary from few 100s of femtoseconds (fs) to 2 ps. Hence, these findings suggest that the reaction conditions that stabilize the charge transferred to OH would facilitate the Cl_2 formation. This leads to the next section of the study depicting the effect of addition of proton on the reaction.

We investigated the HOCl + Cl$^-$ → Cl_2 + OH$^-$ also with small water cluster model of 6 water molecules. Water cluster results indicate that the pre-reactive halogen bonded complexes are thermodynamically more stable than the product state. The calculations were carried out by using the MP2/6-311++G**//PBE0-D/6-31+G* method (Figure S5). The results revealed a mechanism where the formation of a Cl_2 molecule occurs through a proton transfer process from one of the water molecules to a hydroxide fragment in the HOCl molecule. Interestingly, the stability of the post-reaction complex was observed only under specific conditions, where the Cl_2 molecule and OH$^-$ ion were separated by multiple water molecules. In contrast, when the separation distance was insufficient, the formation of the Cl_2 product molecule could not be achieved.

Effect of Proton (Low pH) on the Cl_2 Formation Reaction. Chemical reactions influenced by acidity have a significant

https://doi.org/10.1021/acs.jpclett.3c03035
J. Phys. Chem. Lett. 2024, 15, 432−438

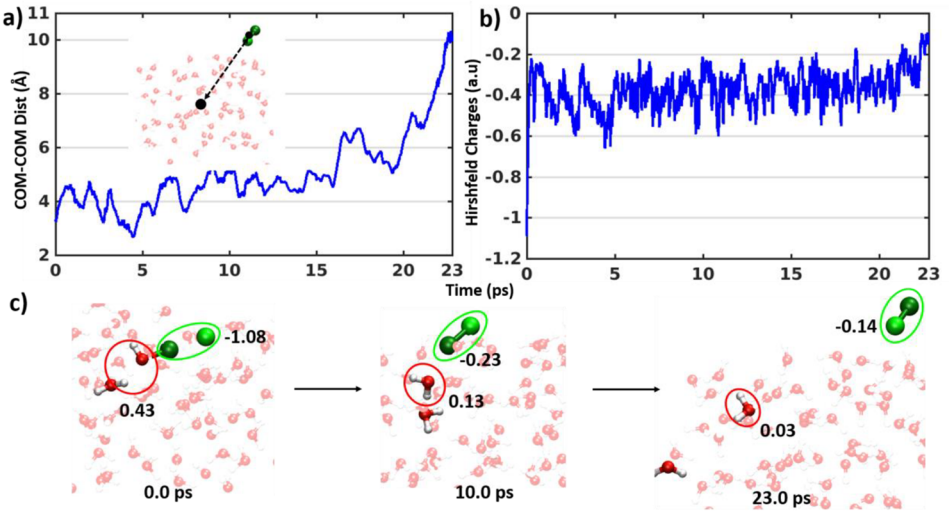

Figure 4. (a and b) Time evolution of the distance between geometric center of the water slab and the formed Cl_2 (*inset*) and Hirshfeld partial charge (summation of Cl^- and Cl from HOCl) of halogen bonded $(HOCl)\cdots(Cl^-)_{aq}$ complexes along trajectory. (c) Snapshots of the halogen bonded $(HOCl)\cdots(Cl^-)_{aq}$ complexes with hydronium ion at different time steps with the Hirshfeld charges of Cl_2 and H_2O are mentioned on those.

effect on the tropospheric multiphase oxidant budget. Here, we investigate the effect of acidity on the Cl_2 formation reaction and mimic the acidity or low pH of the water medium by adding a proton to a neighboring water molecule forming hydronium ion. Our simulations with hydronium ion indicate that $HOCl + Cl^- + H^+ \rightarrow Cl_2 + H_2O$ reaction proceeds via a mechanism where the proton reacts with halogen bonded $(HOCl)\cdots(Cl^-)_{aq}$ complex. Figure 3c shows the time evolution of the bond lengths related to the Cl_2 and H_2O formation reaction. The $Cl{-}Cl^-$ bond length decreases to 2.0 Å (blue) and the Cl−O bond length increases (red) at the same time (black line) indicating the Cl_2 formation. The Hirshfeld partial charge analysis also reveals a similar transition in the same time region around 100 fs (black line). The partial charge on the Cl^- (light green) ion got transferred to OH (red) and form neutral H_2O (Figure 3d). The O−H bond length (green in Figure 3c), which depicts the bond distance between the O atom of HOCl moiety and one H of the hydronium ion, also indicates the formation of H_2O. Data from the whole ∼20 ps simulation (Figure S6 and Figure 4) shows that Cl_2 formation is nonreversible and will not revert to a halogen bonded $(HOCl)\cdots(Cl^-)_{aq}$ complex. The time evolution of the distance between the geometric center of the water box and the geometric center of the Cl_2 formed (Figure 4a) reveals that after 20 ps Cl_2 would detach from the slab. The Hirshfeld partial charge analysis also suggests that Cl_2 loses all interactions with all neighboring atoms leading to complete neutral partial charge for Cl_2 (Figure 4b). Data pertaining to simulations resulting nonreversible Cl_2 are provided in Figure S7 and simulation leading to the detachment of Cl_2 can be found in Figure S8. The enhancement of the heterogeneous Cl_2 formation reaction in acidic environment collaborated well with laboratory experiments[21] and field observations.[19,22]

As during the Cl_2 formation in acidic medium, the extra proton departs from the hydronium ion and effectively attaches to OH forming a H_2O (water), the correct alignment of one of the protons of the hydronium ion to OH of HOCl is crucial. 2D potential energy scan (Figure 5) along the distance (r) between the closest proton of OH to the O atom and angle to

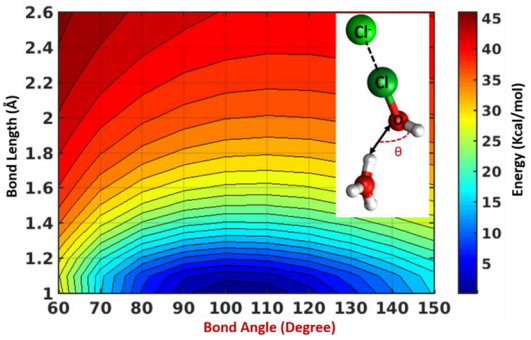

Figure 5. 2D potential energy scan along bond length between O atom of HOCl (r) and proton from hydronium ion and θ (description in text) for halogen bonded $(HOCl)\cdots(Cl^-)_{aq}$ complexes in acidic pH.

be formed between OH and proton (θ) shows a minimum suggesting preorganization of hydronium ion. This result indicates that one of the protons of the hydronium ion must be within a distance of less than 2 Å from the transiently generated hydroxide ion. Moreover, the Cl_2 formation highly depends on the specific orientation of the hydronium ion, and the θ angle to be formed during the process requires to be ∼80−120° angle (Figure 5). These findings align with previous research for bromide radical formation[34] and proton transfer process in water medium.[35] These studies demonstrated the significant role of relative orientations of the reactants in facilitating their entrance into the "cone of acceptance", which is compatible with the formation of the specific HOH angle of the product water molecule. In our simulations also, we observe that when the dynamics is started with $\theta \sim 80{-}120°$ (Table S2) that leading to the formation of the bond angle of water (∼104°), the system transitions to products in less than 300 fs (Figure 3 and Figure S7). Other θ orientations are not exhibiting any reaction in the simulation time scale.

In this study, we establish the atomistic mechanism of the $HOCl + Cl^- \rightarrow Cl_2 + OH^-$ reaction at the air−water interface. Initially, the reaction proceeds by the formation of pre-reactive complexes of $(HOCl)\cdots(Cl^-)_{aq}$ surrounded with the neighbor-

https://doi.org/10.1021/acs.jpclett.3c03035
J. Phys. Chem. Lett. 2024, 15, 432−438

ing water molecules. Both the hydrogen bonded complex and the halogen bonded complex are thoroughly investigated in the study. Our simulations reveal the significant role of the halogen bonded $(HOCl)\cdots(Cl^-)_{aq}$ complex in the process of atmospheric Cl_2 formation. The substantial lifetime of 20 ps, for the halogen bonded complexes in water at neutral pH suggests that their role as reaction precursors in the chemistry of aqueous environments may be more critical than conventionally assumed. The Cl_2 formation reaction proceeds by halogen bonded complexes of $(HOCl)\cdots(Cl^-)_{aq}$ surrounded with the neighboring water molecules and undergo charge transfer from Cl^- to OH^- to form transient Cl_2 at neutral pH. Addition of a proton to one proximal water greatly facilitates the Cl_2 formation which explains the enhanced experimental rate at low pH. Indeed, this proton addition mimicking the low pH experimental condition stabilizes the charge on OH^- forming neutral H_2O (water). Furthermore, the specific orientation of the nearest proton of hydronium ion to OH of HOCl is essential for the reaction to proceed. Moreover, because of the increased entropy effect due to water formation, the reaction is expected to be enhanced at the interface with respect to bulk. On the other hand, despite the sufficient lifetime of the hydrogen bonded $(HOCl)\cdots(Cl^-)_{aq}$ complexes in water, those remain unreactive throughout simulations. In a parallel study on halogen bonded complexes of $(HOCl)\cdots(I^-)_{aq}$ from our lab establish the pivotal role of halogen bonded complexes in the halogen exchange reaction $HOCl + I^- \rightarrow HOI + Cl^-$. This study also highlights the enormous enhancement in the reaction rate compared to that in the gas phase reaction due to the catalytic effect of the waters from the slab. In summary, our study suggests the desirability of future investigations of the potential role of halogen-bonded complexes of halogen-containing molecules as precursors or intermediates in various atmospheric reactions at air−water interfaces or in a water medium. These studies also unveil some atmospheric implications such as (1) at acidic aqueous environments (aerosol, seawater) dihalogen formation would be dominant, whereas at neutral pH halogen exchange would play a significant role. This would have substantial consequences for the dihalogen and hypohalous acid distribution in the atmosphere.

COMPUTATIONAL METHODS

DFT Calculations:Gas-phase optimization and 2D Potential Energy Scan. Minimum energy structures of $(HOCl)\cdots(Cl^-)$ complex in gas phase are calculated using method B3LYP[36] and def2-TZVPD basis.[37] We perform a 2D potential energy scan along the distance between the closest proton of OH to O atom and angle to be formed between OH and proton (θ) using PBE exchange correlation functional[38] and cc-PVDZ basis set. All the single point calculations with opt = modred option are implemented in Gaussian 16, Revision C.01.[39]

Ab Initio Molecular Dynamics (AIMD) Simulations with Water Slab. We adopt similar procedures for our simulations utilized by the Gerber group in several previous publications[23,25] to describe chemical reactions on water slab. The unit cell of the slab is modeled by 72 water molecules in a $13.47 \times 15.56 \times 40$ Å^3 rectangular box. Periodic boundary conditions are employed in x and y but not in the z direction, mimicking the water surface in the xy plane. A water molecule at the center of the box is replaced with the gas phase optimized $(HOCl)\cdots(Cl^-)$ complex. The system is then equilibrated at 300 K for ∼3.0 ps using a Nosé−Hoover massive thermostat,[40] with a 0.5 fs time step until the $(HOCl)\cdots(Cl^-)$ complex reaches to the topmost layer of the water slab. Subsequently, these systems are simulated for 20 ps, resulting in the formation of the halogen and hydrogen bonded $(HOCl)\cdots(Cl^-)_{aq}$ complexes. From the second step 10 simulations for halogen bonded $(HOCl)\cdots(Cl^-)_{aq}$ complexes and 5 simulations for hydrogen bonded $(HOCl)\cdots(Cl^-)_{aq}$ complexes are performed for 20 ps initializing with different velocities using different SEED parameter in CP2K 7.1.[41] Similarly, we introduce one extra proton to neighboring water forming hydronium ion for the simulations mimicking acidic pH. The protons are incorporated to the water in the structures derived from the neutral pH simulations, where one proton of water is in a specific angle orientation as discussed above (*vide supra*). Considering the fast nature of proton transfer from hydronium to OH of HOCl, we employ 0.2 fs time step for first 4 ps. Subsequently, the time step is increased to 0.5 fs for the rest of the simulations.

All ab initio molecular dynamics simulations are performed using the QUICKSTEP module[42] of CP2K 7.1[41] employing Perdew−Burke−Ernzerhof density functional[38] with a Grimme dispersion correction (PBE-D3).[43,44] Previous study from our group with this DFT potential for this type of charge transfer reactions supports the reliability in this study.[23] Double-zeta valence polarization basis-set (DZVP-MOLOPT-SR)[45] and the Goedecker−Teter−Hutter (GTH) pseudopotentials[46] are employed for the computations. We treat the long-range electrostatic interactions using the Martyna−Tuckerman algorithm.[47] For the plane-wave basis set, a cutoff of 320 Ry (1 Ry = 1.097×10^7 m^{-1}) is employed, along with a relative cutoff of 50 Ry. All hydrogen atoms are substituted by deuterium to accommodate a larger time step of 0.5 fs for simulations. This choice is substantiated, as nuclear quantum effects are not anticipated to have a substantial impact on the properties detailed in this section.

In our analysis, we examine the Hirshfeld charges[33] generated from CP2K 7.1.[41] This charge analysis is based on the concept of describing the molecule by dividing it into its constituent atoms and gauging how these atoms deviate from the isolated atoms. Accordingly, the molecular density at each point for the individual atoms within the molecule is allocated in proportion to their respective contributions to the promolecule density at that point. The promolecular density is a direct sum of free contributions from all constituent atoms of the molecule. This charge analysis is shown to accurately describe the charge transfer reactions in water clusters,[48,49] providing a well-suited approach for defining similar reactions in our system of interest.

Water Cluster Calculations. To better understand the mechanisms of Cl_2 formation during the interaction HOCl with Cl^- ion at water surface, the reaction $HOCl + Cl^- \rightarrow Cl_2 + OH^-$ in the presence of 6 water molecules was simulated. Ab initio quantum-chemical methods were applied such as the calculations of potential energy surfaces (PESs), determinations of transition states (TSs), and intrinsic reaction coordinate procedure (IRC). The PESs were initially studied using the PBE0 hybrid functional[50] and 6-31+G* basis set using the Q-Chem[51] and GAMESS[52] programs. It has been shown that the PBE0 functional works well for water clusters and ion−water systems.[53] Additionally, the DFT-D2 dispersion correction from Grimme is used.[54] Energy for obtained structures were recalculated with MP2/6-311++G** level of theory. The number of negative eigenvalues of the Hessian

https://doi.org/10.1021/acs.jpclett.3c03035
J. Phys. Chem. Lett. 2024, 15, 432−438

matrix was examined for all of the stationary points. Additionally, zero-point energies, enthalpies, and Gibbs free energies (at 298 K) were used for thermochemical analysis. All resulting TSs were linked to their corresponding PES minima by descending along the reaction coordinate using the Gonzalez–Schlegel algorithm (IRC).[55]

■ ASSOCIATED CONTENT

Supporting Information

The Supporting Information is available free of charge at https://pubs.acs.org/doi/10.1021/acs.jpclett.3c03035.

Additional data showing geometric and electronic properties along trajectories, Figures S1–S8 and Tables S1 and S2 (PDF)

Transparent Peer Review report available (PDF)

■ AUTHOR INFORMATION

Corresponding Author

R. Benny Gerber − *The Fritz Haber Center for Molecular Dynamics, Institute of Chemistry, The Hebrew University of Jerusalem, Jerusalem 91904, Israel; Department of Chemistry, University of California, Irvine, California 92697, United States;* orcid.org/0000-0001-8468-0258; Email: robertbenny.gerber@mail.huji.ac.il

Authors

Imon Mandal − *The Fritz Haber Center for Molecular Dynamics, Institute of Chemistry, The Hebrew University of Jerusalem, Jerusalem 91904, Israel;* orcid.org/0000-0001-9680-8407

Natalia V. Karimova − *Department of Chemistry, University of California, Irvine, California 92697, United States;* orcid.org/0000-0002-4616-1884

Itai Zakai − *The Fritz Haber Center for Molecular Dynamics, Institute of Chemistry, The Hebrew University of Jerusalem, Jerusalem 91904, Israel;* orcid.org/0000-0002-0543-6562

Complete contact information is available at: https://pubs.acs.org/10.1021/acs.jpclett.3c03035

Notes

The authors declare no competing financial interest.

■ ACKNOWLEDGMENTS

The authors would like to thank Professor Mark Johnson, Professor Gilbert Nathanson, and Professor Tim Bertram for helpful discussions. The work was supported by U.S. National Science Foundation Center for Aerosol Impacts on Chemistry of the Environment (NSF-CAICE) CHE-1801971; The Advanced Cyberinfrastructure Coordination Ecosystem: Services and Support (ACCESS) program and SDSC EXPANSE CPU through the TG-CHE170064 allocation; and The Israel Science Foundation (ISF) grant 593/20.

■ REFERENCES

(1) Saiz-Lopez, A.; von Glasow, R. Reactive halogen chemistry in the troposphere. *Chem. Soc. Rev.* **2012**, *41*, 6448–6472.

(2) Tilgner, A.; Schaefer, T.; Alexander, B.; Barth, M.; Collett, J. L.; Fahey, K. M.; Nenes, A.; Pye, H. O. T.; Herrmann, H.; McNeill, V. F. Acidity and the multiphase chemistry of atmospheric aqueous particles and clouds. *Atmos. Chem. Phys.* **2021**, *21*, 13483–13536.

(3) Sherwen, T.; Schmidt, J. A.; Evans, M. J.; Carpenter, L. J.; Grossmann, K.; Eastham, S. D.; Jacob, D. J.; Dix, B.; Koenig, T. K.; Sinreich, R.; et al. Global impacts of tropospheric halogens (Cl, Br, I) on oxidants and composition in GEOS-Chem. *Atmos. Chem. Phys.* **2016**, *16*, 12239–12271.

(4) Simpson, W. R.; Brown, S. S.; Saiz-Lopez, A.; Thornton, J. A.; von Glasow, R. Tropospheric Halogen Chemistry: Sources, Cycling, and Impacts. *Chem. Rev.* **2015**, *115*, 4035–4062.

(5) Schmidt, J. A.; Jacob, D. J.; Horowitz, H. M.; Hu, L.; Sherwen, T.; Evans, M. J.; Liang, Q.; Suleiman, R. M.; Oram, D. E.; Le Breton, M.; et al. Modeling the observed tropospheric BrO background: Importance of multiphase chemistry and implications for ozone, OH, and mercury. *J. Geophys. Res. Atmos.* **2016**, *121*, 11819–11835.

(6) Hoffmann, E. H.; Tilgner, A.; Vogelsberg, U.; Wolke, R.; Herrmann, H. Near-Explicit Multiphase Modeling of Halogen Chemistry in a Mixed Urban and Maritime Coastal Area. *ACS Earth Space Chem.* **2019**, *3*, 2452–2471.

(7) Parrella, J. P.; Jacob, D. J.; Liang, Q.; Zhang, Y.; Mickley, L. J.; Miller, B.; Evans, M. J.; Yang, X.; Pyle, J. A.; Theys, N.; et al. Tropospheric bromine chemistry: implications for present and pre-industrial ozone and mercury. *Atmos. Chem. Phys.* **2012**, *12*, 6723–6740.

(8) Ariya, P. A.; Amyot, M.; Dastoor, A.; Deeds, D.; Feinberg, A.; Kos, G.; Poulain, A.; Ryjkov, A.; Semeniuk, K.; Subir, M.; et al. Mercury Physicochemical and Biogeochemical Transformation in the Atmosphere and at Atmospheric Interfaces: A Review and Future Directions. *Chem. Rev.* **2015**, *115*, 3760–3802.

(9) Carpenter, L. J.; MacDonald, S. M.; Shaw, M. D.; Kumar, R.; Saunders, R. W.; Parthipan, R.; Wilson, J.; Plane, J. M. C. Atmospheric iodine levels influenced by sea surface emissions of inorganic iodine. *Nat. Geosci.* **2013**, *6*, 108–111.

(10) Sherwen, T.; Evans, M. J.; Carpenter, L. J.; Schmidt, J. A.; Mickley, L. J. Halogen chemistry reduces tropospheric O_3 radiative forcing. *Atmos. Chem. Phys.* **2017**, *17*, 1557–1569.

(11) von Glasow, R.; Sander, R.; Bott, A.; Crutzen, P. J. Modeling halogen chemistry in the marine boundary layer - 1. Cloud-free MBL. *J. Geophys. Res. Atmos.* **2002**, *107*, ACH9-1–ACH9-16.

(12) Finlayson-Pitts, B. J.; Ezell, M. J.; Pitts, J. N. Formation of Chemically Active Chlorine Compounds by Reactions of Atmospheric NaCl Particles with Gaseous N_2O_5 and $ClONO_2$. *Nature* **1989**, *337*, 241–244.

(13) Keene, W. C.; Sander, R.; Pszenny, A. A. P.; Vogt, R.; Crutzen, P. J.; Galloway, J. N. Aerosol pH in the marine boundary layer: A review and model evaluation. *J. Aerosol Sci.* **1998**, *29*, 339–356.

(14) Vogt, R.; Crutzen, P. J.; Sander, R. A mechanism for halogen release from sea-salt aerosol in the remote marine boundary layer. *Nature* **1996**, *383*, 327–330.

(15) von Glasow, R.; Sander, R.; Bott, A.; Crutzen, P. J. Modeling halogen chemistry in the marine boundary layer - 2. Interactions with sulfur and the cloud-covered MBL. *J. Geophys. Res. Atmos.* **2002**, *107*, ACH2-1–ACH2-12.

(16) Hoffmann, E. H.; Tilgner, A.; Wolke, R.; Herrmann, H. Enhanced Chlorine and Bromine Atom Activation by Hydrolysis of Halogen Nitrates from Marine Aerosols at Polluted Coastal Areas. *Environ. Sci. Technol.* **2019**, *53*, 771–778.

(17) Angle, K. J.; Crocker, D. R.; Simpson, R. M. C.; Mayer, K. J.; Garofalo, L. A.; Moore, A. N.; Mora Garcia, S. L.; Or, V. W.; Srinivasan, S.; Farhan, M.; et al. Acidity across the interface from the ocean surface to sea spray aerosol. *Proc. Natl. Acad. Sci. U.S.A.* **2021**, *118*, e2018397118.

(18) Sommariva, R.; von Glasow, R. Multiphase Halogen Chemistry in the Tropical Atlantic Ocean. *Environ. Sci. Technol.* **2012**, *46*, 10429–10437.

(19) Lawler, M. J.; Sander, R.; Carpenter, L. J.; Lee, J. D.; von Glasow, R.; Sommariva, R.; Saltzman, E. S. HOCl and Cl_2 observations in marine air. *Atmos. Chem. Phys.* **2011**, *11*, 7617–7628.

(20) Deborde, M.; von Gunten, U. Reactions of chlorine with inorganic and organic compounds during water treatment - Kinetics and mechanisms: A critical review. *Water Res.* **2008**, *42*, 13–51.

(21) Wren, S. N.; Donaldson, D. J.; Abbatt, J. P. D. Photochemical chlorine and bromine activation from artificial saline snow. *Atmos. Chem. Phys.* **2013**, *13*, 9789−9800.
(22) Newberg, J. T.; Matthew, B. M.; Anastasio, C. Chloride and bromide depletions in sea-salt particles over the northeastern Pacific Ocean. *J. Geophys. Res. Atmos.* **2005**, *110* (D6), D06209.
(23) Hirshberg, B.; Rossich Molina, E.; Götz, A. W.; Hammerich, A. D.; Nathanson, G. M.; Bertram, T. H.; Johnson, M. A.; Gerber, R. B. N_2O_5 at water surfaces: binding forces, charge separation, energy accommodation and atmospheric implications. *Phys. Chem. Chem. Phys.* **2018**, *20*, 17961−17976.
(24) Partanen, L.; Murdachaew, G.; Gerber, R. B.; Halonen, L. Temperature and collision energy effects on dissociation of hydrochloric acid on water surfaces. *Phys. Chem. Chem. Phys.* **2016**, *18*, 13432−13442.
(25) Murdachaew, G.; Nathanson, G. M.; Gerber, R. B.; Halonen, L. Deprotonation of formic acid in collisions with a liquid water surface studied by molecular dynamics and metadynamics simulations. *Phys. Chem. Chem. Phys.* **2016**, *18*, 29756−29770.
(26) Gerber, R. B.; Varner, M. E.; Hammerich, A. D.; Riikonen, S.; Murdachaew, G.; Shemesh, D.; Finlayson-Pitts, B. J. Computational Studies of Atmospherically-Relevant Chemical Reactions in Water Clusters and on Liquid Water and Ice Surfaces. *Acc. Chem. Res.* **2015**, *48*, 399−406.
(27) Stropoli, S. J.; Khuu, T.; Messinger, J. P.; Karimova, N. V.; Boyer, M. A.; Zakai, I.; Mitra, S.; Lachowicz, A. L.; Yang, N.; Edington, S. C.; et al. Preparation and Characterization of the Halogen-Bonding Motif in the Isolated Cl^-·IOH Complex with Cryogenic Ion Vibrational Spectroscopy. *J. Phys. Chem. Lett.* **2022**, *13*, 2750−2756.
(28) Stropoli, S. J.; Khuu, T.; Boyer, M. A.; Karimova, N. V.; Gavin-Hanner, C. F.; Mitra, S.; Lachowicz, A. L.; Yang, N.; Gerber, R. B.; McCoy, A. B.; et al. Electronic and mechanical anharmonicities in the vibrational spectra of the H-bonded, cryogenically cooled X^-· HOCl (X = Cl, Br, I) complexes: Characterization of the strong anionic H-bond to an acidic OH group. *J. Chem. Phys.* **2022**, *156*, 174303.
(29) Arunan, E.; Desiraju, G. R.; Klein, R. A.; Sadlej, J.; Scheiner, S.; Alkorta, I.; Clary, D. C.; Crabtree, R. H.; Dannenberg, J. J.; Hobza, P.; et al. Definition of the hydrogen bond (IUPAC Recommendations 2011). *Pure Appl. Chem.* **2011**, *83*, 1637−1641.
(30) Desiraju, G. R.; Ho, P. S.; Kloo, L.; Legon, A. C.; Marquardt, R.; Metrangolo, P.; Politzer, P.; Resnati, G.; Rissanen, K. Definition of the halogen bond (IUPAC Recommendations 2013). *Pure Appl. Chem.* **2013**, *85*, 1711−1713.
(31) Chen, H.; Varner, M. E.; Gerber, R. B.; Finlayson-Pitts, B. J. Reactions of Methanesulfonic Acid with Amines and Ammonia as a Source of New Particles in Air. *J. Phys. Chem. B* **2016**, *120*, 1526−1536.
(32) Dawson, M. L.; Varner, M. E.; Perraud, V.; Ezell, M. J.; Wilson, J.; Zelenyuk, A.; Gerber, R. B.; Finlayson-Pitts, B. J. Amine-Amine Exchange in Aminium-Methanesulfonate Aerosols. *J. Phys. Chem. C* **2014**, *118*, 29431−29440.
(33) Hirshfeld, F. L. Bonded-atom fragments for describing molecular charge densities. *Theor. Chim. Acta* **1977**, *44*, 129−138.
(34) Coutinho, N. D.; Aquilanti, V.; Silva, V. H. C.; Camargo, A. J.; Mundim, K. C.; de Oliveira, H. C. B. Stereodirectional Origin of anti-Arrhenius Kinetics for a Tetraatomic Hydrogen Exchange Reaction: Born-Oppenheimer Molecular Dynamics for OH + HBr. *J. Phys. Chem. A* **2016**, *120*, 5408−5417.
(35) Tuckerman, M.; Laasonen, K.; Sprik, M.; Parrinello, M. Ab Initio Molecular Dynamics Simulation of the Solvation and Transport of H_3O^+ and OH^- Ions in Water. *J. Phys. Chem.* **1995**, *99*, 5749−5752.
(36) Becke, A. D. Density functional thermochemistry. III. The role of exact exchange. *J. Chem. Phys.* **1993**, *98*, 5648−5652.
(37) Rappoport, D.; Furche, F. Property-optimized Gaussian basis sets for molecular response calculations. *J. Chem. Phys.* **2010**, *133*, 134105.
(38) Perdew, J. P.; Burke, K.; Ernzerhof, M. Generalized Gradient Approximation Made Simple. *Phys. Rev. Lett.* **1996**, *77*, 3865−3868.
(39) *Gaussian 16 Rev. C.01*; Gaussian: Wallingford, CT, 2019.
(40) Martyna, G. J.; Klein, M. L.; Tuckerman, M. Nosé-Hoover chains: The canonical ensemble via continuous dynamics. *J. Chem. Phys.* **1992**, *97*, 2635−2643.
(41) Kühne, T. D.; Iannuzzi, M.; Del Ben, M.; Rybkin, V. V.; Seewald, P.; Stein, F.; Laino, T.; Khaliullin, R. Z.; Schütt, O.; Schiffmann, F.; et al. CP2K: An electronic structure and molecular dynamics software package - Quickstep: Efficient and accurate electronic structure calculations. *J. Chem. Phys.* **2020**, *152*, 194103.
(42) VandeVondele, J.; Krack, M.; Mohamed, F.; Parrinello, M.; Chassaing, T.; Hutter, J. Quickstep: Fast and accurate density functional calculations using a mixed Gaussian and plane waves approach. *Comput. Phys. Commun.* **2005**, *167*, 103−128.
(43) Grimme, S.; Antony, J.; Ehrlich, S.; Krieg, H. A consistent and accurate ab initio parametrization of density functional dispersion correction (DFT-D) for the 94 elements H-Pu. *J. Chem. Phys.* **2010**, *132*, 154104.
(44) Grimme, S.; Ehrlich, S.; Goerigk, L. Effect of the damping function in dispersion corrected density functional theory. *J. Comput. Chem.* **2011**, *32*, 1456−1465.
(45) VandeVondele, J.; Hutter, J. Gaussian basis sets for accurate calculations on molecular systems in gas and condensed phases. *J. Chem. Phys.* **2007**, *127*, 114105.
(46) Goedecker, S.; Teter, M.; Hutter, J. Separable dual-space Gaussian pseudopotentials. *Phys. Rev. B* **1996**, *54*, 1703−1710.
(47) Martyna, G. J.; Tuckerman, M. E. A reciprocal space based method for treating long range interactions in ab initio and force-field-based calculations in clusters. *J. Chem. Phys.* **1999**, *110*, 2810−2821.
(48) Mitra, S.; Denton, J. K.; Kelleher, P. J.; Johnson, M. A.; Guasco, T. L.; Choi, T. H.; Jordan, K. D. Water Network Shape-Dependence of Local Interactions with the Microhydrated -NO_2^- and -CO_2^- Anionic Head Groups by Cold Ion Vibrational Spectroscopy. *J. Phys. Chem. A* **2022**, *126*, 2471−2479.
(49) Khuu, T.; Schleif, T.; Mohamed, A.; Mitra, S.; Johnson, M. A.; Valdiviezo, J.; Heindel, J. P.; Head-Gordon, T. Intra-cluster Charge Migration upon Hydration of Protonated Formic Acid Revealed by Anharmonic Analysis of Cold Ion Vibrational Spectra. *J. Phys. Chem. A* **2023**, *127*, 7501−7509.
(50) Adamo, C.; Barone, V. Toward reliable density functional methods without adjustable parameters: The PBE0 model. *J. Chem. Phys.* **1999**, *110*, 6158−6170.
(51) Shao, Y.; Gan, Z.; Epifanovsky, E.; Gilbert, A. T. B.; Wormit, M.; Kussmann, J.; Lange, A. W.; Behn, A.; Deng, J.; Feng, X.; et al. Advances in molecular quantum chemistry contained in the Q-Chem 4 program package. *Mol. Phys.* **2015**, *113*, 184−215.
(52) Schmidt, M. W.; Baldridge, K. K.; Boatz, J. A.; Elbert, S. T.; Gordon, M. S.; Jensen, J. H.; Koseki, S.; Matsunaga, N.; Nguyen, K. A.; Su, S.; et al. General atomic and molecular electronic structure system. *J. Comput. Chem.* **1993**, *14*, 1347−1363.
(53) Karimova, N. V.; Chen, J.; Gord, J. R.; Staudt, S.; Bertram, T. H.; Nathanson, G. M.; Gerber, R. B. S_N2 Reactions of N_2O_5 with Ions in Water: Microscopic Mechanisms, Intermediates, and Products. *J. Phys. Chem. A* **2020**, *124*, 711−720.
(54) Grimme, S. Semiempirical GGA-type density functional constructed with a long-range dispersion correction. *J. Comput. Chem.* **2006**, *27*, 1787−1799.
(55) Gonzalez, C.; Schlegel, H. B. Reaction path following in mass-weighted internal coordinates. *J. Phys. Chem.* **1990**, *94*, 5523−5527.

https://doi.org/10.1021/acs.jpclett.3c03035
J. Phys. Chem. Lett. 2024, 15, 432−438